

Accepted Manuscript

Divergent regulation of insulin-like growth factor binding protein genes in cultured Atlantic salmon myotubes under different models of catabolism and anabolism

Daniel Garcia de la Serrana, Eduardo N. Fuentes, Samuel A.M. Martin, Ian A. Johnston, Daniel J. Macqueen

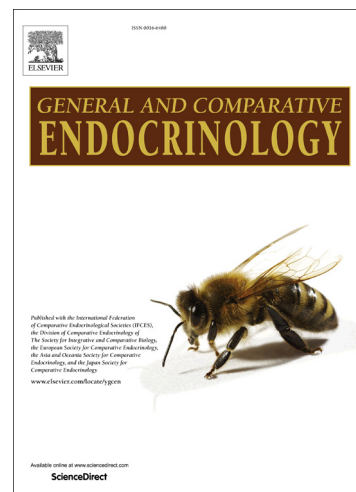
PII: S0016-6480(16)30399-9
DOI: <http://dx.doi.org/10.1016/j.ygcen.2017.01.017>
Reference: YGCEN 12565

To appear in: *General and Comparative Endocrinology*

Received Date: 18 November 2016
Revised Date: 12 January 2017
Accepted Date: 17 January 2017

Please cite this article as: Garcia de la Serrana, D., Fuentes, E.N., Martin, S.A.M., Johnston, I.A., Macqueen, D.J., Divergent regulation of insulin-like growth factor binding protein genes in cultured Atlantic salmon myotubes under different models of catabolism and anabolism, *General and Comparative Endocrinology* (2017), doi: <http://dx.doi.org/10.1016/j.ygcen.2017.01.017>

This is a PDF file of an unedited manuscript that has been accepted for publication. As a service to our customers we are providing this early version of the manuscript. The manuscript will undergo copyediting, typesetting, and review of the resulting proof before it is published in its final form. Please note that during the production process errors may be discovered which could affect the content, and all legal disclaimers that apply to the journal pertain.



1 **Divergent regulation of insulin-like growth factor binding protein genes in cultured**
2 **Atlantic salmon myotubes under different models of catabolism and anabolism**

3

4 Daniel Garcia de la Serrana ^{*^ a}, Eduardo N. Fuentes ^{^a,b,c}, Samuel A.M. Martin ^c, Ian A. Johnston ^a,
5 Daniel J. Macqueen ^{* c}

6

7 ^a School of Biology, Scottish Oceans Institute, University of St Andrews, Fife KY16 8LB, Scotland,
8 United Kingdom.

9

10 ^b Interdisciplinary Center for Aquaculture Research (INCAR), Víctor Lamas 1290, PO Box 160-C,
11 Concepción, Chile.

12

13 ^c Institute of Biological and Environmental Sciences, University of Aberdeen, Tillydrone Avenue,
14 Aberdeen, AB24 2TZ, Scotland, United Kingdom.

15

16 * Corresponding authors:

17 Daniel Garcia de la Serrana. Email address: dgdisc@st-andrews.ac.uk

18 Daniel J. Macqueen. Email address: daniel.macqueen@abdn.ac.uk

19 [^]Authors contributed equally

20 **Running title:** Igfbp expression and remodelling of fish myotubes

21

22

23

24

25

26

27 **Abstract**

28

29 Much attention has been given to insulin-like growth factor (Igf) pathways that regulate the balance
30 of skeletal muscle protein synthesis and breakdown in response to a range of extrinsic and intrinsic
31 signals. However, we have a less complete understanding of how the same signals modulate muscle
32 mass upstream of such signalling, through a family of functionally-diverse Igf-binding proteins
33 (Igfbps) that modify the availability of Igfs to the cell receptor Igf1r. We exposed cultured myotubes
34 from Atlantic salmon (*Salmo salar* L.) to treatments recapturing three catabolic signals: inflammation
35 (interleukin-1 β), stress (dexamethasone) and fasting (amino acid deprivation), plus one anabolic
36 signal: recovery of muscle mass post-fasting (supplementation of fasted myotubes with Igf-I and
37 amino acids). The intended phenotype of treatments was confirmed by significant changes in
38 myotube diameter and immunofluorescent staining of structural proteins. We quantified the mRNA-
39 level regulation of the full expressed Igf and Igfbp gene complement across a post-treatment time
40 course, along with marker genes for muscle structural protein synthesis, as well as muscle
41 breakdown, via the ubiquitin-proteasome and autophagy systems. Our results highlight complex, non-
42 overlapping responses of Igfbp family members to the different treatments, suggesting that the profile
43 of expressed Igfbps is differentially regulated by distinct signals promoting similar muscle
44 remodelling phenotypes. We also demonstrate divergent regulation of salmonid-specific gene
45 duplicates of *igfbp5b1* and *igfbp5b2* under distinct catabolic and anabolic conditions. Overall, this
46 study increases our understanding of the regulation of Igfbp genes in response to signals that promote
47 remodelling of skeletal muscle.

48

49 **Keywords:** Skeletal muscle, Myotubes, Cell culture, Insulin-like growth factor system; Igf binding
50 proteins, Atlantic salmon, Dexamethasone, Interleukin-1 β , amino acids.

51

52

53 1. Introduction

54

55 Skeletal muscle growth involves a net accumulation of protein, with rates of protein synthesis
56 exceeding that of degradation. One of the key systems regulating this balance is the insulin-like
57 growth factor (Igf) - phosphoinositide 3 kinase (Pi3k) - Akt/protein kinase B (Akt) - mammalian
58 target of rapamycin (mTor) pathway. The hormones Igf-I and Igf-II act as endocrine factors (Laron,
59 1996; Wood et al. 2005), but are also released locally by tissues, including skeletal muscle
60 (Schiaffino and Mammucari, 2011). Both Igfs are major anabolic factors in skeletal muscle,
61 promoting protein synthesis, whilst inhibiting atrophy (Firth and Baxter 2002; Wood et al., 2005;
62 Duan et al., 2010). The binding of Igf hormones to Igf1r, their primary cell-membrane receptor,
63 initiates an intracellular phosphorylation cascade that activates Pi3k complexes and key downstream
64 signalling molecules, most notably Akt (Hers et al., 2011), which in turn activates mTor/Raptor
65 complexes – inducing an increase in protein translation via regulation of P70s6 kinases and Eif4ebp1
66 family members (Wang and Proud, 2006). Regulation of Igfs in the extracellular environment (e.g.
67 circulation and extracellular matrix) provides an important level of upstream control to these
68 signalling events and is primarily governed by a family of functionally-diverse Igf binding proteins
69 (Igfbp-1 to 6) present in all vertebrates, but particularly well-characterized in mammals. These Igfbps
70 can either restrict Igf hormones from Igf1r or facilitate the accumulation of Igf on cell membranes in
71 proximity to Igf1r (Firth and Baxter, 2002; Duan and Xu, 2005). Accordingly, the expression of
72 different Igfbp subtypes allows for both inhibition and potentiation of Igf-signalling, which may
73 allow appropriate muscle mass regulation according to signals favouring catabolism or anabolism.

74

75 The ubiquitin-proteasome and autophagy-lysosome systems are major pathways leading to skeletal
76 muscle protein degradation (Schiaffino et al., 2013). The ubiquitin-proteasome pathway is crucial for
77 removal of sarcomeric proteins following muscle damage, in response to changes in muscle activity,
78 or upon remodelling of muscle mass (Murton et al., 2008). Proteins to be degraded by the proteasome

79 are cross-linked by muscle-specific E3-ubiquitin ligases to ubiquitin (Schiaffino et al., 2013). The
80 main recognized E3-ubiquitin ligases in skeletal muscle, employed widely as markers of muscle
81 catabolism, are F-box only protein 32 (Fbxo32) (also called Atrogin-1 or Mafbx) and members of the
82 muscle RING-finger (Murf) family (Glass 2005, Satchek et al., 2007; Johnston et al. 2011;
83 Macqueen et al. 2014). The autophagy-lysosome pathway also plays a key role in the turnover of
84 cellular organelles during both normal and stressful conditions (Schiaffino et al., 2013). The Igf
85 pathway negatively regulates both degradation pathways through activated Akt, which
86 phosphorylates Foxo transcription factors, blocking their nuclear entry (Tzivion et al., 2011), causing
87 downregulation of target genes including *mafbx* and *murfl* (Glass, 2005), as well as key genes
88 involved in lysosome formation and autophagy (Mammucari et al., 2007). The impact of external and
89 endogenous signals driving skeletal muscle breakdown on these intracellular pathways is well
90 characterized (Bonaldo and Sandri, 2013). For example, glucocorticoids such as the cortisol-analogue
91 dexamethasone, increase the transcription of *murfl*, *mafbx* and autophagy genes, while inhibiting
92 protein synthesis by blocking mTor function (Braun and Marks, 2015). In addition, cytokines, such as
93 *Tnfa* and $IL-1\beta$ increase the transcription of E3-ubiquitin ligases, including *murfl* via $Nfk\beta$ pathways
94 (Glass, 2005; Pooley et al., 2013). Finally, fasting stimulates protein degradation by repressing Akt
95 activation, leading to FoxO-mediated transcriptional upregulation of both E3-ubiquitin ligases and
96 macro-autophagy genes (e.g. Sandri et al., 2004; Southgate et al., 2007; Calnan and Brunet, 2008;
97 Seiliez et al. 2010; Shimizu et al., 2011).

98
99 Comparatively less is known about the role of Igfbps in skeletal muscle under such catabolic signals,
100 particularly in teleost fish, where remodelling of muscle mass occurs routinely during the life cycle
101 for reallocation of energy and amino acids between tissues (Johnston et al., 2011). For example,
102 many teleosts undergo seasonal cycles of muscle wasting associated with migration and/or the
103 mobilisation of amino acids to build gonadal tissue, followed by recovering after spawning (e.g.
104 James and Johnston, 1998; Mommsen, 2004). Interestingly, in teleosts the Igfbp family is

105 characterized by additional gene duplicates (paralogues) of Igfbp1-6 retained from a whole genome
106 duplication (WGD) event ancestral to all teleosts (i.e. Igfbp1a/b, 2a/b, 3a/b, 5a/b and 6a/b) (Ocampo
107 Daza et al. 2011; Johnston et al. 2011; Macqueen et al. 2013). Additionally, in the salmonid family of
108 teleosts (the focus of the current study), the Igfbp family consists of no less than nineteen unique
109 genes (Macqueen et al. 2013; Lappin et al. 2016), owing to the retention of additional paralogues
110 from a salmonid-specific WGD ~95 Ma (Macqueen and Johnston, 2014; Lien et al. 2016). This event
111 has also expanded other components of the IGF system, including Igf1r (Alzaid et al. 2016a) and Igf-
112 II in some species (Lappin et al. 2016). Recent work on salmonid Igfbps in skeletal muscle has
113 included studies of *in vitro* regulation during myogenesis under anabolic and catabolic signals
114 (Gabillard et al. 2006; Bower and Johnston, 2010; Pooley et al. 2013) and *in vivo* regulation in
115 response to fasting (e.g. Bower et al., 2008), temperature (Hevrøy et al., 2013) and sex steroids
116 (Cleveland and Weber, 2015). Moreover, the salmonid Igfbp subtypes *igfbp1a1* and *igfbp6a2* have
117 roles linking salmonid growth to conserved cytokine pathways regulating inflammatory responses
118 (Alzaid et al. 2016b), with relevance to understanding muscle remodelling for energy reallocation
119 (Pooley et al. 2013). In contrast, the regulation of Igfbps by dexamethasone (or other glucocorticoids)
120 in fish skeletal muscle remains unstudied.

121

122 The objective of this study was to improve our understanding of how the Igfbp gene family is
123 regulated by a range of physiological stimuli known to induce remodelling of skeletal muscle mass.
124 We quantified the transcriptional responses of the complete repertoire of expressed Igfbps in primary
125 differentiated fast-twitch skeletal muscle cultures from Atlantic salmon (*Salmo salar* L.) using four
126 experimental models that induced a catabolic or anabolic status, via pathways regulated by
127 dexamethasone, proinflammatory cytokines, amino acids and Igf-I. Our results show distinct stimuli
128 result in divergent and complex expression responses of Igfbp family member genes during muscle
129 remodelling, including evolutionary divergence of salmonid-specific gene duplicates.

130

131 2. Materials and Methods

132

133 2.1. Ethics statement

134 The University of St Andrews Animal Ethics and Welfare Committee approved all the experimental
135 procedures described. Fish were sacrificed by a blow to the head before sectioning of the spinal cord
136 (Schedule-1 killing protocol; Animals Act 1986; Home Office Code of Practice. HMSO: London
137 January 1997).

138

139 2.2. Myotube cell culture

140 Atlantic salmon (*Salmo salar* L.) were maintained at the Scottish Oceans Institute (University of St
141 Andrews) in 200L fibreglass freshwater tanks at 10°C with a 16:8 light/dark photoperiod. Myogenic
142 progenitor cells (MPCs) were extracted from 10-14g Atlantic salmon parr (immature fish of unknown
143 sex) and cell culture performed as previously described (Garcia de la serrana and Johnston, 2013).
144 Briefly, epaxial fast skeletal muscle was extracted (total 40g of muscle, n=10 to 14 randomly-
145 sampled fish per culture), mechanically dissected and enzymatically digested with trypsin and
146 collagenase, then washed and filtered several times until MPCs were obtained. Cells were cultured in
147 laminin-coated well plates and maintained with Dulbecco's modified eagle's media (DMEM; Sigma,
148 Dorset, UK), 9mM NaHCO₃ (pH 7.4) (Sigma), 20mM HEPES (Sigma), 10% (v/v) foetal bovine
149 serum (Sigma) and an antibiotic/antimycotic cocktail (Sigma) at 18°C for 10 days until fully
150 differentiated myotubes were formed.

151

152 2.3. Experimental treatments

153 Catabolic and anabolic treatments were performed in day-10 differentiated Atlantic salmon myotubes
154 in independent cultures (n=5). Catabolism was induced by addition of 1µM of dexamethasone
155 (+DEX treatment) (Sigma), 3ng/ml of recombinant interleukin-1β (produced following Hong et al.
156 2001) (+IL-1β treatment) or using an amino acid free cell culture media (-AA treatment). In order to

157 establish conditions that induced myotube atrophy without affecting cell viability, dexamethasone
158 and IL-1 β concentrations were obtained from the literature (Menconi et al., 2008; Pooley et al., 2013)
159 and a pilot study was carried out to test different concentrations (data not shown). Myotubes were
160 incubated in bovine serum free media for two hours to reduce gene expression to basal levels before
161 +DEX and +IL-1 β treatments. Total RNA was extracted (section 2.4) at 0, 1, 3, 6, 24 and 48 hours
162 post-treatment. For the AA- treatment, a modified culture media with no amino acids was used
163 (Garcia de la serrana and Johnston, 2013) and total RNA extracted at 0, 1, 3, 6, 24 and 48 hours. The
164 anabolic treatment (+AA+Igf-I) involved a restitution of amino acids in the -AA cell culture media
165 (at 48 hours) combined with 100nM of recombinant Atlantic salmon Igf-I (GROPEP, Australia).
166 Total RNA from the +AA+Igf-I treatment was collected 3, 6 and 24 hours after the +AA+Igf-I
167 treatment. In all cases, myotubes with normal free-serum DMEM media were maintained in parallel
168 as controls (-DEX, -IL-1 β , +AA and +AA-Igf-I) for each of the conditions tested and sampled at the
169 same time as treated cells.

170

171 **2.4. RNA extraction and cDNA synthesis**

172 Total RNA was extracted from two wells per time-point, per treatment and culture using an RNeasy
173 extraction kit (Qiagen, Manchester, UK), following the manufacturers protocol. RNA concentrations,
174 230/260 and 280/260 ratios were determined using a Nanodrop 1000 spectrophotometer (Nanodrop,
175 ThermoFisher Scientific). RNA with respective 260/280 and 260/280 ratios over 1.8 and 2 was used
176 for cDNA synthesis. 250ng of RNA was reverse transcribed for each sample using a Quantitech kit
177 (Qiagen), following the manufacturers guidelines, including a step to remove residual genomic DNA.
178 Control samples with RNA but no reverse transcriptase (-RT) were included. The 1:1 first-strand
179 cDNA was diluted 40x and stored at -20°C until use in quantitative PCR (qPCR) (section 2.6). A pool
180 of all first-strand cDNAs generated was used as an interplate calibrator (IPC) for qPCR analysis
181 (section 2.6).

182

183 2.5. Primer design

184 Primers used for amplification of the complete salmonid Igfbp family (19 genes), as well as *maf**bx*,
185 *mur**f1*, *igf2*, *myl1*, *tnn1* and the housekeeping genes *hprt1*, *rpl4*, *rps13*, *rps29* have been described
186 elsewhere (Bower et al., 2008; Macqueen et al., 2010; 2013; Alzaid et al., 2016b). New primers for
187 paralogues encoding autophagy related 4b cysteine protease (*atg4b*) genes were designed for use in
188 this study. First, BLASTn searches of the Atlantic salmon genome (via Salmobase.org) revealed two
189 *atg4b* paralogues on Chr. 10 and 16 (respective NCBI accession numbers: NM_001139775 and
190 XM_014149865), embedded within a large collinear duplicated block retained from the salmonid
191 specific WGD (Lien et al. 2016). These salmonid-specific paralogues were named *atg4b1* (Chr. 10)
192 and *atg4b2* (Chr. 16). Primers designed to be specific to each gene are as follows (underlined bases
193 distinguish the two paralogues): *atg4b1* - Fwd: 5' – GACTGGAGATGGGTGAGGAGC – 3'
194 (melting temperature, T_m = 61 °C); Rev: 5' – CCGTTAGGCTCTGGCATACC – 3' (T_m = 60 °C)
195 (product size = 382 bp) and *atg4b2* - Fwd: 5' – GAGACTGGAGATGGGTGAGAGG – 3' (T_m = 60
196 °C); Rev: 5' – GGCAGCCGTTATGCGTCG – 3' (T_m = 63 °C) (product size = 340 bp). For both
197 *atg4b* paralogues, the primers in a pair were separated by at least three exons in the gene.

198

199 2.6. qPCR analysis

200 All qPCR experiments were compliant with MIQE guidelines (Bustin et al., 2009). Each reaction
201 contained 6µl of 1:40-diluted cDNA, 7.5µl of 2x Brilliant III SYBRGreen master mix (Agilent,
202 Cheshire, UK) and 1.5µl of sense/antisense 500nM primer mix. Amplifications were performed in
203 duplicate in a Stratagene Mx3005P thermocycler (Agilent) with the following conditions: 3 min at
204 95°C, followed by 40 cycles of 20s at 95°C then 20s at 65°C, followed by a dissociation analysis
205 (60°C to 95°C thermal gradient; single product observed in all final assays). No-template (-NT; water
206 in place of cDNA) and -RT controls were included in duplicate for each qPCR assay. The IPC cDNA
207 sample was included in quadruplicate using the same primer pair (*rps29*) on every qPCR plate.
208 Threshold crossing/quantification cycles (C_q) were calculated from baseline-corrected data with the

209 threshold fixed across plates at 0.25. Cq-36 was considered the cut-off of no expression (note: Cq
210 was always >40 for -RT and -NTC controls). LinRegPCRv.11 software was used to calculate primer
211 efficiency following the author's recommendations (Ruijter et al. 2009). Cq values were exported to
212 Genex v.4.4.2 (MultiD Analyses AB) and corrected for differences in efficiency before any plate-to-
213 plate variation was corrected using the IPC Cq values.

214

215 An assessment of reference gene suitability was performed using Normfinder (Andersen et al. 2004)
216 within Genex. Normfinder was used to consider variance in expression of the four reference genes
217 both globally and across the post-treatment time courses (considering controls vs. treatments). This
218 was done with pooled cDNAs for each biological replicate (separate pools of replicates for +DEX, -
219 DEX, +IL-1 β , -IL-1 β , -AA +AA, +AA+Igf1 and +AA-Igf1) and sampling points (0, 1, 3, 6, 24, and
220 48h) (n=42 sample points) providing a study-wide overview of reference gene stability. We also
221 performed a Normfinder analysis of all four reference genes considering the Dexamethasone study
222 with full biological replication (n=60 samples; -DEX and +DEX across 6 timepoints). Each of the
223 four reference genes were expressed very stably in the pooled samples, both globally and with respect
224 to treatment and time-point (Normfinder SD values: 0.17-0.22). The Dexamethasone data revealed
225 that *rps29*, *rps13* and *rpl4* were stably expressed (global Normfinder SD values of 0.06-0.20), with
226 *rps29* being the most stable. Importantly, the accumulative SD of reference genes, which is
227 indicative of the appropriate number of reference genes to employ for normalization, was not lowered
228 (improved) by considering additional reference genes to *rps29*. Thus, using Genex, we normalized
229 the efficiency-corrected Cq values for all experimental genes measured across the study to the
230 relevant *rps29* Cq values, before placing the expression data on a relative scale quantitatively
231 comparable across all experimental genes.

232

233 **2.7. Muscle fibre diameter and immunofluorescence measurements**

234

235 To measure myotube diameter and perform immunofluorescence detection, MPCs were grown on
236 borosilicate coverslips coated with poly-L-lysine and laminin until fusion. Diameter was measured in
237 10-day differentiated myotubes from all tested treatments. Culture media was removed 24 and 48
238 hours after myotubes were incubated with the different treatments and control media, and washed
239 twice with PBS. Duplicate coverslips for each time-point (24h and 48h; treatment and controls) were
240 fixed in 4% (m/v) paraformaldehyde (Sigma) in PBS (pH 7.4) for 20 minutes at room temperature,
241 washed twice with PBS and kept at 4°C in a solution of PBS 0.01% NaN₃ (Sigma) until further
242 analysis. Photographs were taken at random for each time-point, treatment and culture (n=4 in each
243 case), using a bright field microscope at 20x magnification. ImageJ software (National Institute of
244 Health, Maryland, USA) was used to determine myotube diameter by measuring the thickness at 5
245 different locations along the myotube. Measurements were obtained from between 15 and 30
246 randomly selected myotubes. Final myotube diameter was taken as the average of the 5
247 measurements (100 to 150 myotubes per treatment/relevant controls).

248

249 Immunofluorescence against actin and desmin filaments was visualised based on a protocol outlined
250 previously (Garcia de la serrana and Johnston, 2013). Fixed myotubes were washed twice in PBS and
251 incubated with 0.5% Triton X-100 (v/v) (Sigma) PBS for 5 min. Non-specific binding sites were
252 blocked with 5% (v/v) normal goat serum (Sigma), 1.5% (w/v) Bovine serum albumin (Sigma), 0.1%
253 (v/v) Triton X-100 (v/v) PBS for 1 hour at room temperature. Actin filaments were visualized by
254 incubation with Phalloidin-ATTO 488 antibody (Sigma) for 2 hours at room temperature at 1:100
255 dilution in 1.5% BSA (w/v) 0.1% Triton X-100 (v/v) PBS and counterstained with DAPI 1:500 in
256 sterile water for 5 minutes. Desmin filaments were detected by incubating the cells with an anti-
257 Desmin antibody (SIGMA) 1:20 (v/v) in 1.5% BSA 0.1% Triton X-100 PBS overnight at 4°C. To
258 visualize the filaments, myotubes were incubated with anti-rabbit Alexa Fluor 546 (ThermoFisher)
259 secondary antibody at 1:400 (v/v) dilution in 1.5% BSA 0.1% Triton X-100 for 2 hours at room
260 temperature and counterstained with DAPI 1:500 in sterile water for 5 minutes. Myotubes were

261 visualized and digitally imaged using a Leica TCS SP2 confocal microscope (Leica Microsystems) at
262 20x magnification.

263

264 **2.8. Statistical analysis**

265 All statistical analyses were performed using RStudio (RStudio Team 2015). Pairwise comparisons of
266 myotube diameter between treatments and controls were done using a Student's t-test. For analysis of
267 the gene expression data, a general linear model approach was used with *treatment* and *time-point* as
268 fixed factors. The Shapiro-Wilk test was used to scrutinize the assumption of normality in the linear
269 model residuals. Expression data that failed to follow a normal distribution was transformed using a
270 Box-Cox power transformation and tested again. Data that did not follow normality after Box-Cox
271 power transformation was analysed using a Kruskal-Wallis non-parametric test.

272

273 **3. Results**

274

275 **3.1. Effect of catabolic and anabolic treatments on myotube diameter**

276 The effect of the different treatments on salmon myotube morphology and cytoskeleton arrangement
277 was assessed 24 and 48 hours after treatment using bright field microscopy and immunofluorescence
278 against actin and desmin filaments (Figure 1A; Supplementary File 1). After 48 hours treatment, each
279 tested catabolic treatment caused a reduction in the number of differentiated myotubes and an
280 increase in the presence of single cells, evidenced both by bright microscopy (Figure 1A, i-k vs.
281 control data in a-c) and desmin immunofluorescence (Figure 1A, m-o vs. control data in e-g).
282 Considering that we used differentiated myotubes as the starting point for each treatment, a reduction
283 in the number of myotubes, coupled with an increase in the number of single cells, might be
284 explained by a dramatic reduction in the integrity of the myotube cytoskeleton. In other words, the
285 apparent single cells may actually remain part of myotubes where the cytoskeleton has undergone
286 extensive atrophy. Bright-field microscopy (Figure 1A, d, i) and desmin immunofluorescence (Figure

287 1A, h, p) showed that the addition of amino acids and Igf-I (+AA+Igf) to myotubes under amino acid
288 deprivation for 48h (-AA-48h) (Figure 1A, d, h) induced myotube hypertrophy (Figure 1A, i, p).

289

290 To quantify the accompanying phenotypic changes in myotubes, we compared myotube diameters for
291 all treatments against controls. +DEX and -AA treatments reduced myotube diameter by ~30-40% at
292 24 and 48 hours compared to controls (all $P < 0.001$) (Figure 1B and C). The +IL-1 β treatment
293 reduced myotube diameter by ~10% at 24 hours ($P = 0.055$) and by ~30% at 48 hours ($P < 0.001$)
294 (Figure 1D). When amino acids and Igf-I were added to the -AA culture (-48h time-point), myotube
295 diameter increased to pre-treatment values in 24h ($P < 0.001$) (Figure 1B). These data confirm that
296 the treatments induced the intended myotube phenotypic changes, which provides a robust platform
297 to interpret gene expression responses measured in the same experimental samples (section 3.2).

298

299 3.2. Gene expression responses to catabolic and anabolic stimuli

300 Genes encoding all 19 Igfbps were quantified using qPCR in Atlantic salmon myotubes, but 10 were
301 not detected, namely *igfbp1a2*, *igfbp1b1*, *igfbp2b1*, *igfbp2b2*, *igfbp3a2*, *igfbp3b1*, *igfbp3b2*, *igfbp6a2*
302 and *igfbp6b1*. Given that the relevant primers have been verified in past studies where expression of
303 all 19 genes was reported (e.g. Macqueen et al. 2013; Alzaid et al. 2016b), we concluded that these
304 *igfbp* genes were not expressed in salmon myotubes. In parallel, genes encoding two E3-ubiquitin
305 ligases (*mafbx*, *murf1*), two fast-twitch skeletal muscle sarcomere components (myosin light chain,
306 *myl1* and troponin I, *tnni1*), the Igf-II hormone (*igf2*) and two autophagy related genes (*atg4b1*,
307 *atg4b2*) were also analysed.

308

309 3.2.1. +DEX treatment

310 10 of the 16 tested genes were significantly regulated by the +DEX treatment compared to controls
311 ($P < 0.05$ for *treatment* effect), including those encoding 6 of the 10 expressed Igfbp family members,
312 both tested E3 Ubiquitin ligases, one of the *atg4b* paralogues and *igf2* (Table 1). In addition, 4 of the

313 10 genes with a significant treatment effect showed a significant *treatment*time-point* interaction,
314 indicating marked differences in the response to dexamethasone at different time-points (Table 1).
315 Among these were two genes encoding Igfbp6 family members (*igfbp6a1* and *igfbp6b2*), which
316 showed reciprocal responses across the treatment time course. Specifically, comparing +DEX to
317 control cultures, *igfbp6a1* was most highly downregulated, while *igfbp6b2* was most highly
318 upregulated at later time-points (24 to 48 hours) of the culture (Figure 2A, B), where atrophy was
319 evident (Figure 1B-D). A similar pattern was observed for two Igfbp5 family members, with *igfbp5a*
320 being downregulated at 24 to 48 hours post treatment and *igfbp5b1* being strongly induced from 6
321 hours post-treatment (Figure 2C, D). The other two Igfbp family members that responded
322 significantly to the +DEX treatment (*igfbp4* and *igfbp2a*) showed a less pronounced trend in the
323 nature and magnitude of response across time-points (Figure 2E, F). The two E3 Ubiquitin ligase
324 genes showed highly distinct responses to the +DEX treatment (Figure 2G, H). Specifically, *mafbx*
325 was induced from early stages of the culture (before notable changes in myotube diameter were
326 observed), through to 24 hours, when atrophy was first observed (Figure 1C) but returned to control
327 levels by 48 hours (Figure 2G). Conversely, *murfl* was induced relative to control levels at 24 and 48
328 hours sampling points (Figure 2H). In addition, both *igf2* and *atgb42* were markedly induced at 24
329 and 48 hours post +DEX treatment (Figure 2I, H).

330

331 Therefore, the most pronounced changes in gene expression responses to dexamethasone occurred at
332 stages of the culture (post-6 hours), when myotube remodelling was evident.

333

334 3.2.3. +IL-1 β treatment

335 Despite our observation that myotube diameter decreased significantly in response to the +IL-1 β
336 treatment by 48 hours (Figure 1D), only 2 of the 16 tested genes were significantly regulated during
337 this remodelling of myotube phenotype (Table 2; Figure 3). This included *igfbp1a1*, which was

338 downregulated at 3, 6 and 48 hours post-treatment, but not other time-points (Table 2; Figure 3A). In
339 contrast, *murfl* was increased in response to controls, most notably at 48 hours (Figure 3B).

340

341 3.2.4. -AA treatment

342 The -AA treatment was accompanied by significant responses in only 3 of the 16 tested genes (Table
343 3; Figure 4), despite clear evidence of myotube atrophy (Figure 1B). Two of the genes significantly
344 regulated by the -AA treatment were the same Igfbp6 family members that were strongly affected by
345 dexamethasone (section 3.2.2). Specifically, both *igfbp6a1* and *igfbp6b2* were downregulated during
346 the -AA treatment time course relative to controls (Table 3), with *igfbp6a1* being particularly
347 strongly affected from 6 hours post treatment (Figure 4A, B). The other gene significantly affected by
348 the -AA treatment, *mafbx*, was downregulated at many sampled time-points (Table 3; Figure 4C).

349

350 3.2.5. +AA+Igf-I treatment

351 The +AA+Igf-I treatment, which was accompanied by a significant recovery of myotube diameter
352 (i.e. anabolic state) (Figure 1B), led to significant responses in 8 of the 16 tested genes, including 4
353 encoding Igfbp family members, *mafbx*, *igf2* and both paralogues of *atg4b* (Table 4; Figure 5).
354 Among the significantly responsive Igfbp genes, three were increased, either transiently (*igfbp6b2*,
355 Figure 5A), or consistently across multiple timepoints (*igfbp5b1* and *igfbp4*, Figure 5B, C).
356 Conversely, *igfbp1a1* was downregulated at all timepoints post +AA+Igf-I treatment (Figure 5D).
357 Finally, while *mafbx* and both *atg4b* duplicates were downregulated by the +AA+Igf-I treatment at
358 multiple sampled timepoints, *igf2* was upregulated (Figure 5E-H).

359

360 4. Discussion

361

362 Here we addressed the regulation of Igfbp gene expression in skeletal muscle remodelling, which is
363 poorly understood in teleost fish. Our study is the first to systematically document the regulation of

364 the complete Igfbp gene family under several distinct catabolic and anabolic conditions, done with
365 full knowledge of gene paralogues retained from both the teleost and salmonid-specific WGD events,
366 which if ignored can limit physiological interpretations of gene expression (Johnston et al. 2011).
367 Though all three tested catabolic signals (i.e. dexamethasone, IL-1 β and amino acid deprivation)
368 induced atrophy of differentiated myotubes (Figure 1), the responses of different Igfbp genes, as well
369 as other relevant marker genes, showed remarkable variability across the tested experimental models
370 (Tables 1-3; Figures 2-5). This was true not only for the number of genes showing a significant
371 response (i.e. from only 2 genes responding to IL-1 β , up to 10 to dexamethasone), but also the
372 particular Igfbp genes that responded to different stimuli. This points to complex and context-
373 dependent transcriptional regulation of Igfbp gene expression via several unique pathways that
374 promote muscle remodelling.

375

376 Dexamethasone-induced atrophy of salmon myotubes (Figure 1) was accompanied by a complex
377 expression response of different Igfbp genes (Figure 2). The catabolic state of the myotubes was also
378 evidenced by upregulation of *mafbx*, *murfl* and *atg4b1* (Table 1), suggesting activation of the
379 proteasome and autophagy systems. However, we also observed Igf system expression responses that
380 are difficult to reconcile with a purely catabolic state, particularly the upregulation of *igf2*, *igfbp4* and
381 *igfbp5b1* (Table 1). While past work has showed that *igf2* is likewise induced by dexamethasone in
382 salmonid hepatocytes (Pierce et al. 2010), its protein product, along with Igfbp5, are established pro-
383 myogenic factors in mammals with key roles in differentiation (e.g. Stewart et al. 1996; Ren et al.
384 2008). Similarly, *igfbp4* has pro-growth functions in salmonid muscle (Johnston et al. 2011; e.g.
385 Bower et al. 2008; Macqueen et al. 2011). Despite this, past *in vitro* studies have also shown that both
386 *igf2* and *igfbp5b1* are much more highly expressed in mononuclear MPCs compared to differentiated
387 myotubes, suggesting roles in early phases of myogenesis, such as MPC proliferation (Bower and
388 Johnston, 2010). Additionally, dexamethasone, despite being a potent inducer of atrophy (e.g. Braun
389 and Marks, 2015) has been shown to activate IGF-signalling pathways promoting early phases of

390 myogenesis (Giorgino and Smith, 1995). Thus, some observed Igfbp system expression responses
391 might result from stimulation of such IGF-signalling pathways, despite the overall catabolic status of
392 salmon myotubes.

393

394 The reciprocal responses of two functionally-related Igfbp5 teleost family members to
395 dexamethasone, with *igfbp5a* downregulated and *igfbp5b1* upregulated (Figure 2C, D) is also notable,
396 as past reports have suggested that mammalian Igfbp5, while being essential for mammalian muscle
397 differentiation (Ren et al. 2008), can also inhibit muscle differentiation under some physiological
398 contexts (Ewton et al. 1998). One explanation for our data is that such divergent roles of Igfbp5 have
399 been partitioned to the individual teleost paralogues during evolution. Interestingly, among the other
400 Igfbp genes that responded to dexamethasone, only *igfbp6a1* and *igfbp6b2* were significantly
401 regulated under any other tested atrophy stimulus, specifically in response to amino acid deprivation
402 (discussed further below). Even then, while *igfbp6a1* was downregulated under both conditions,
403 consistent with a common underlying role, *igfbp6b2* was upregulated by dexamethasone, but
404 downregulated by amino acid deprivation. Moreover, during recovery myotube growth (induced by
405 addition of amino acids and Igf-I to cell cultures previously deprived of amino acids), *igfbp6b2* was
406 increased (i.e. as observed for dexamethasone) despite the myotube showing an anabolic rather than
407 catabolic status. The role of Igfbp6 in teleost muscle remodelling is clearly complex (discussed
408 below), both in response to dexamethasone and other signals, and warrants further study.

409

410 In contrast to dexamethasone, IL-1 β -induced myotube atrophy was not accompanied by marked
411 changes in the expression of Igfbp family members and other tested genes (Table 2). This contrasts
412 two past studies where a much higher dose of IL-1 β was administered to Atlantic salmon myocytes
413 previously cultured for 4 days (25 ng/ml dose; Pooley et al. 2013) or 7 days (50-200 ng/ml dose;
414 Heidari et al. 2016) and several Igfbp genes were strongly affected (Pooley et al. 2013), including the
415 robust induction of an undefined Igfbp6 family member (Pooley et al. 2013; Heidari et al. 2016).

416 However, as we cultured myocytes for 10 days before IL-1 β treatment, our study represents a more
417 advanced state of differentiation (Bower et al., 2010; Bower and Johnston, 2010; Garcia de la serrana
418 et al., 2013). Thus, the discrepancies between our study and these past investigations presumably
419 reflect differences in both the concentrations of IL-1 β used, but potentially also the ontogeny of the
420 cell culture. Interestingly, in another study, a strong upregulation of *Igfbp6a2* was observed in
421 rainbow trout (*Oncorhynchus mykiss*) following *in vivo* bacterial challenge at the fry stage, a response
422 that was strikingly correlated to that of master genes regulated by proinflammatory cytokine
423 pathways, including *IL-1 β* (Alzaid et al. 2016b). However, in that past study, the tissues responsible
424 for *igfbp6a2* upregulation were not determined and whether skeletal muscle was involved remains
425 unknown. In our study, *igfbp1a2* (the single Igfbp1 family member expressed in myotubes) was
426 slightly downregulated in response to IL-1 β (Table 2). However, its salmonid-specific paralogue
427 *igfbp1a2* is robustly induced during bacterial infection, which is presumed to restrict Igf hormones in
428 the circulation (Alzaid et al. 2016b), consistent with past studies showing that salmonid Igfbp1 family
429 members are upregulated in circulation in response to catabolic physiological states (e.g. Kawaguchi
430 et al. 2015). Thus, the downregulation of *igfbp1a2* in atrophic salmon myotubes points to differences
431 in the local and systematic roles of Igfbp1 family members of teleosts. In addition, past work
432 documented a minor induction of *mafbx* in response to IL-1 β in salmon myocytes (Pooley et al.
433 2013), which, again was not detected in our study. However, *murfl*, another E3-Ubiquitin ligase, was
434 upregulated (Table 2). Past reports in mammal myotubes has shown that both E3-Ubiquitin ligases
435 are stimulated by IL-1 β through NF- κ B signalling pathways (e.g. Li et al. 2009).
436

437 As for IL-1 β , we observed a paucity of transcriptional responses in atrophic salmon myotubes
438 deprived of amino acids (Table 3), similar to previous reports (Bower and Johnston, 2010). However,
439 a separate past study showed that the E3-Ubiquitin ligase *mafbx* was robustly induced by the same
440 treatment (Bower et al. 2010), which was not observed in our data. The only other genes that
441 responded to amino acid deprivation were *igfbp6a1* and *igfbp6b2* (Figure 4A, B), which were each

442 strongly decreased, which contrasts with the fact that Igfbp6 is a negative regulator of Igf signalling,
443 particularly through Igf-II, which in mammals binds Igfbp6 with much higher affinity than Igf-I
444 (Bach, 2016). Thus, we suggest that the complex expression responses of different Igfbp6 family
445 members observed in our study, with both positive and negative regulation in myotubes under
446 verified catabolic states is likely related to the plethora of characterized cellular actions for Igfbp6
447 that are IGF-independent (Bach, 2016).

448

449 A stronger expression response for the tested genes was observed during myotube recovery growth
450 induced by amino acids and Igf-I treatment in previously-fasted salmon myotubes, including
451 downregulation of *mafbx* and both *atg4b* paralogues, suggesting repression of the proteasome and
452 autophagy pathways. A concurrent upregulation of several Igf system genes that are considered pro-
453 myogenic, including *igf2*, *igfbp5b1* and *igfbp4*, was also consistent with the observed anabolic state
454 of myotubes and highly congruent with past data using a similar experimental model (Bower et al.,
455 2008). However, the strong episodic upregulation of *igfbp6b2* in response to the +AA+Igf-I treatment
456 (Figure 6A) has not been observed before and will warrant further investigation, especially in light of
457 the diverse expression responses of Igfbp6 family members observed in our broader study.

458

459 A final discussion point is the differential expression of salmonid-specific paralogues in our study.
460 Past work has emphasized the enormous extent of transcriptional divergence that has evolved among
461 such duplicates since the salmonid WGD ~95 Ma, which has been previously demonstrated both at
462 the genome-wide level (across tissues; Lien et al. 2016) and for important gene families in response
463 to various physiological stimuli (e.g. Macqueen et al. 2010; Garcia de la Serrana et al. 2013; Alzaid et
464 al. 2016b). For the Igfbp family, the only such gene duplicates expressed in salmon myotubes were
465 *igfbp5b1* and *igfbp5b2*. In a recent past study, these two genes were shown to have similar regulation
466 during the early development of rainbow trout (Alzaid et al. 2016b). Here, we observed divergent
467 responses of *igfbp5b1* and *igfbp5b2* to dexamethasone (Table 1) and the +AA+Igf-I treatment (Table

468 4), which likely reflects evolutionary divergence in regulatory sequences controlling transcription.
469 Again, such findings emphasize the importance of identifying and distinguishing gene duplicates in
470 investigations of salmonid physiology.

471

472 **5. Conclusion**

473 This study improves our understanding about how a range of stimuli induce catabolic and anabolic
474 status in salmonid myotubes and highlights great evident complexity in the roles played by different
475 Igfbp family members in the control of salmonid skeletal muscle mass.

476

477 **6. Acknowledgements**

478 This work received funding from the MASTS pooling initiative (The Marine Alliance for Science
479 and Technology for Scotland) and their support is gratefully acknowledged. MASTS is funded by the
480 Scottish Funding Council (grant reference HR09011) and contributing institutions.

481

482 **7. Declaration of Interest**

483 The authors declare that they have no competing interests.

484

485 **References**

486

487 Alzaid, A., Martin, S.A., Macqueen, D.J. 2016a. The complete salmonid IGF-IR gene repertoire and
488 its transcriptional response to disease. *Sci Rep.* 6, 34806.

489

490 Alzaid, A., Castro, R., Wang, T., Secombes, C.J., Boudinot, P., Macqueen, D.J., Martin, S.A. 2016b.
491 Cross-talk between growth and immunity: coupling of the insulin-like growth factor axis to
492 conserved cytokine pathways in rainbow trout. *Endocrinology.* 157, 1942-55.

493

- 494 Andersen, C.L., Jensen, J.L., Orntoft, T.F. 2004. Normalization of real-time quantitative reverse
495 transcription-PCR data: a model-based variance estimation approach to identify genes suited for
496 normalization, applied to bladder and colon cancer data sets. *Cancer Res.* 64, 5245-50.
497
- 498 Bach, L.A. 2016. Current ideas on the biology of IGFBP-6: More than an IGF-II inhibitor? *Growth*
499 *Horm IGF Res.* *In press*, pii: S1096-6374(16)30056-9.
500
- 501 Bonaldo, P. and Sandri, M. 2013. Cellular and molecular mechanisms of muscle atrophy. *Dis Model*
502 *Mech.* 6, 25-39.
503
- 504 Bower, N.I., Li, X., Taylor, R., Johnston, I.A. 2008. Switching to fast growth: the insulin-like growth
505 factor (IGF) system in skeletal muscle of Atlantic salmon. *J. Exp Biol.* 211, 3859-3870.
506
- 507 Bower, N.I. and Johnston, I.A. 2010. Transcriptional regulation of the IGF signaling pathway by
508 amino acids and insulin-like growth factors during myogenesis in Atlantic salmon. *PLoS One.* 5,
509 e11100.
510
- 511 Bower N.I., Garcia de la Serrana, D., Johnston, I.A. 2010. Characterisation and differential regulation
512 of MAFbx/Atrogin-1 alpha and beta transcripts in skeletal muscle of Atlantic salmon (*Salmo salar*).
513 *Biochem Biophys Res Commun.* 396, 265-71.
514
- 515 Bustin, S.A., Benes, V., Garson, J.A., Hellemans, J., Huggett, J., Kubista, M., Mueller, R., et al.
516 2009. The MIQE guidelines: minimum information for publication of quantitative real-time PCR
517 experiments. *Clin Chem.* 55, 611-22.
518

- 519 Braun, T.P. and Marks, D.L. 2015. The regulation of muscle mass by endogenous glucocorticoids.
520 Front Physiol. 3, 6-12.
521
- 522 Calnan, D. R. and Brunet, A. 2008. The FoxO code. *Oncogene* 27, 2276–2288.
523
- 524 Cleveland, B.M. and Weber, G.M. 2015. Effects of sex steroids on expression of genes regulating
525 growth-related mechanisms in rainbow trout (*Oncorhynchus mykiss*). *Gen Comp Endocrinol.*
526 216,103-15.
527
- 528 Duan, C. and Xu, Q. 2005. Roles of insulin-like growth factor (IGF) binding proteins in regulating
529 IGF actions. *Gen Comp Endocrinol.* 142, 44-52.
530
- 531 Duan, C., Ren, H., Gao, S. 2010. Insulin-like growth factors (IGFs), IGF receptors, and IGF-binding
532 proteins: roles in skeletal muscle growth and differentiation. *Gen Comp Endocrinol.* 167, 344-51.
533
- 534 Ewton, D.Z., Coolican, S.A., Mohan, S., Chernausk, S.D., Florini, J.R. 1998. Modulation of insulin-
535 like growth factor actions in L6A1 myoblasts by insulin-like growth factor binding protein (IGFBP)-
536 4 and IGFBP-5: a dual role for IGFBP-5. *J Cell Physiol.* 177, 47-57.
537
- 538 Firth, S.M. and Baxter, R.C. 2002. Cellular actions of the insulin-like growth factor binding proteins.
539 *Endocr Rev.* 23, 824-54.
540
- 541 Gabillard, J.C., Kamangar, B.B., Montserrat, N. 2006. Coordinated regulation of the GH/IGF system
542 genes during refeeding in rainbow trout (*Oncorhynchus mykiss*). *J Endocrinol.* 191, 15-24.
543

- 544 Garcia de la serrana, D. and Johnston, I.A. 2013. Expression of heat shock protein 90 (Hsp90)
545 paralogues is regulated by amino acids in skeletal muscle of Atlantic salmon. PLoS ONE. 8, e74295.
546
- 547 Giorgino, F. and Smith, R.J. 1995. Dexamethasone enhances insulin-like growth factor-I effects on
548 skeletal muscle cell proliferation. Role of specific intracellular signaling pathways. J Clin Invest. 96,
549 1473-83.
550
- 551 Glass, D.J. 2005. Skeletal muscle hypertrophy and atrophy signaling pathways. Int J Biochem Cell
552 Biol. 37, 1974-84.
553
- 554 Heidari, Z., Bickerdike, R., Tinsley, J., Zou, J., Wang, T.Y., Chen, T.Y., Martin, S.A. 2016.
555 Regulatory factors controlling muscle mass: competition between innate immune function and
556 anabolic signals in regulation of atrogen-1 in Atlantic salmon. Mol Immunol. 67, 341-9.
557
- 558 Hers, I., Vincent, E.E., Tavaré J.M. 2011. Akt signalling in health and disease. Cell Signal. 23, 1515-
559 27.
560
- 561 Hevrøy, E.M., Hunskaar, C., de Gelder, S., Shimizu, M., Waagbø, R., Breck, O., Takle, H., et al. 2013.
562 GH-IGF system regulation of attenuated muscle growth and lipolysis in Atlantic salmon reared at
563 elevated sea temperatures. J Comp Physiol B. 183, 243-59.
564
- 565 Hong, S., Zou, J., Crampe, M., Peddie, S., Scapigliati, G., Bols, N., Cunningham, C., et al. 2001. The
566 production and bioactivity of rainbow trout (*Oncorhynchus mykiss*) recombinant IL-1 beta. Vet
567 Immunol Immunopathol. 81, 1-14.
568

- 569 James, R.S. and Johnston I.A. 1998. Influence of spawning on swimming performance and muscle
570 contractile properties in the short-horn sculpin. *J Fish Biol.* 53, 485-501.
571
- 572 Johnston, I.A., Bower, N.I., Macqueen, D.J. 2011. Growth and the regulation of myotomal muscle
573 mass in teleost fish. *J Exp Biol.* 214, 1617-1628.
574
- 575 Kawaguchi, K., Kaneko, N., Fukuda, M., Nakano, Y., Kimura, S., Hara, A., Shimizu, M. 2015.
576 Responses of insulin-like growth factor (IGF)-I and two IGF-binding protein-1 subtypes to fasting
577 and re-feeding, and their relationships with individual growth rates in yearling masu salmon
578 (*Oncorhynchus masou*). *Comp Biochem Physiol A Mol Integr Physiol.* 165, 191-8
579
- 580 Laron, Z. 1996. The somatostatin-GHRH-GH-IGF axis. In: Merimee T, Laron Z eds. Growth
581 hormone, IGF-I and growth: new views of old concepts. Modern endocrinology and diabetes, Vol. 4.
582 London-Tel Aviv: Freund Publishing House Ltd. Pp 5–10.
583
- 584 Lappin, F.M., Shaw, R.L., Macqueen, D.J. 2016. Targeted sequencing for high-resolution
585 evolutionary analyses following genome duplication in salmonid fish: Proof of concept for key
586 components of the insulin-like growth factor axis. *Mar Genomics.* *In press*, doi:
587 10.1016/j.margen.2016.06.003.
588
- 589 Li, W., Moylan, J.S., Chambers, M.A., Smith, J., Reid, M.B. 2009. Interleukin-1 stimulates
590 catabolism in C2C12 myotubes. *Am J Physiol Cell Physiol.* 297, C706-14.
591
- 592 Lien, S., Koop, B.F., Sandve, S.R., Miller, J.R., Kent, M.P., Nome, T., Hvidsten, T.R., et al. 2016.
593 The Atlantic salmon genome provides insights into rediploidization. *Nature.* 533, 200-5.
594

- 595 Macqueen, D.J., Kristjánsson, B.K., Johnston, I.A. 2010. Salmonid genomes have a remarkably
596 expanded akirin family, coexpressed with genes from conserved pathways governing skeletal muscle
597 growth and catabolism. *Physiol Genomics*. 42, 134-48.
- 598
- 599 Macqueen, D.J., Kristjánsson, B.K., Paxton, C.G., Vieira, V.L., Johnston, I.A. 2011. The parallel
600 evolution of dwarfism in Arctic charr is accompanied by adaptive divergence in mTOR-pathway
601 gene expression. *Mol Ecol*. 20, 3167-84.
- 602
- 603 Macqueen, D.J., Garcia de la serrana, D., Johnston, I.A. 2013. Evolution of ancient functions in the
604 vertebrate insulin-like growth factor system uncovered by study of duplicated salmonid fish genomes.
605 *Mol Biol Evol*. 30, 1060-76.
- 606
- 607 Macqueen, D.J. and Johnston, I.A. 2014. A well-constrained estimate for the timing of the salmonid
608 whole genome duplication reveals major decoupling from species diversification. *Proc Biol Sci*. 281,
609 1778.
- 610
- 611 Macqueen, D.J., Fuentes, E.N., Valdés, J.A., Molina, A., Martin, S.A. 2014. The vertebrate muscle-
612 specific RING finger protein family includes MuRF4--a novel, conserved E3-ubiquitin ligase. *FEBS*
613 *Lett*. 588, 4390-7.
- 614
- 615 Mammucari, C., Milan, G., Romanello, V., Masiero, E., Rudolf, R., Del Piccolo, P., Burden, S.J., et
616 al. 2007. FoxO3 controls autophagy in skeletal muscle in vivo. *Cell Metab*. 6, 458-71.
- 617
- 618 Menconi, M., Gonnella, P., Petkova, V., Lecker, S., Hasselgren, P.O. 2008. Dexamethasone and
619 corticosterone induce similar, but not identical, muscle wasting responses in cultured L6 and C2C12
620 myotubes. *J Cell Biochem*. 105, 353-64.

621

622 Mommsen, T.P. 2004. Salmon spawning migration and muscle protein metabolism: the August
623 Krogh principle at work. *Comp Biochem Physiol B Biochem. Mol Biol.* 139: 383-400.

624

625 Murton, A.J., Constantin, D., Greenhaff, P.L. 2008. The involvement of the ubiquitin proteasome
626 system in human skeletal muscle remodelling and atrophy. *Biochim Biophys Acta.* 1782, 730-43.

627

628 Ocampo Daza, D., Sundström, G., Bergqvist, C.A., Duan, C., Larhammar, D. 2011. Evolution of the
629 insulin-like growth factor binding protein (IGFBP) family. *Endocrinology.* 152, 2278-89.

630

631 Pierce, A.L., Dickey, J.T., Felli, J., Swanson, P., Dickhoff, W.W. 2010. Metabolic hormones regulate
632 basal and growth hormone-dependent igf2 mRNA level in primary cultured coho salmon
633 hepatocytes: effects of insulin, glucagon, dexamethasone, and triiodothyronine. *J Endocrinol.* 204,
634 331-9.

635

636 Pooley, N.J., Tacchi, L., Secombes, C.J., Martin, S.A. 2013. Inflammatory responses in primary
637 muscle cell cultures in Atlantic salmon (*Salmo salar*). *BMC Genomics.* 14, 747.

638

639 Ren, H., Yin, P., Duan C. 2008. IGFBP-5 regulates muscle cell differentiation by binding to IGF-II
640 and switching on the IGF-II auto-regulation loop. *J Cell Biol.* 182, 979-91.

641

642 RStudio Team. 2015. RStudio: Integrated Development for R. RStudio, Inc., Boston, MA.
643 <http://www.rstudio.com/>

644

645 Ruijter, J.M., Ramakers, C., Hoogaars, W., Bakker, O., van den Hoff, M.J.B., Karlen, Y., Moorman,
646 A.F.M. 2009. Amplification efficiency: linking baseline and bias in the analysis of quantitative PCR
647 data. *Nucleic Acids Res.* 37, e45.

648

649 Sacheck, J.M., Hyatt, J.P., Raffaello, A., Jagoe, R.T., Edgerton, V.R., Lecker, S.H., Goldberg, A.L.
650 2007. Rapid disuse and denervation atrophy involve transcriptional changes similar to those of
651 muscle wasting during systemic diseases. *FASEB J.* 21, 140-55.

652

653 Sandri, M., Sandri, C., Gilbert, A., Skurk, C., Calabria, E., Picard, A., Walsh, K., et al. 2004. Foxo
654 transcription factors induce the atrophy-related ubiquitin ligase atrogen-1 and cause skeletal muscle
655 atrophy. *Cell.* 117, 399-412.

656

657 Schiaffino, S. and Mammucari, C., 2011. Regulation of skeletal muscle growth by the IGF1-Akt/PKB
658 pathway: insights from genetic models. *Skelet Muscle.* 4, 18.

659

660 Schiaffino, S., Dyar, K.A., Ciciliot, S., Blaauw, B., Sandri, M. 2013. Mechanisms regulating skeletal
661 muscle growth and atrophy. *FEBS J.* 280, 4294-4314.

662

663 Seiliez, I., Gutierrez, J., Salmerón, C., Skiba-Cassy, S., Chauvin, C., Dias, K., Kaushik, S., et al.
664 2010. An in vivo and in vitro assessment of autophagy-related gene expression in muscle of rainbow
665 trout (*Oncorhynchus mykiss*). *Comp Biochem Physiol B Biochem Mol Biol.* 157, 258-66

666

667 Shimizu, N., Yoshikawa, N., Ito, N., Maruyama, T., Suzuki, Y., Takeda, S., Nakae, J., et al. 2011.
668 Crosstalk between glucocorticoid receptor and nutritional sensor mTOR in skeletal muscle. *Cell*
669 *Metab.* 13, 170–182.

670

671 Southgate, R.J., Neil, B., Prelovsek, O., El-Osta, A., Kamei, Y., Miura, S., Ezaki, O., et al. 2007.
672 FOXO1 regulates the expression of 4E-BP1 and inhibits mTOR signaling in mammalian skeletal
673 muscle. *J Biol Chem.* 282, 21176–21186.
674
675 Stewart, C.E., James, P.L., Fant, M.E., Rotwein, P. 1996. Overexpression of insulin-like growth
676 factor-II induces accelerated myoblast differentiation. *J Cell Physiol.* 169, 23–32.
677
678 Tzivion, G., Dobson, M., Ramakrishnan, G. 2011. FoxO transcription factors; Regulation by AKT
679 and 14-3-3 proteins. *Biochim Biophys Acta.* 1813, 1938-45.
680
681 Wang, X. and Proud, C.G. 2006. The mTOR pathway in the control of protein synthesis. *Physiology*
682 (Bethesda). 21, 362-9.
683
684 Wood, A.W., Duan, C., Bern, H.A. 2005. Insulin-like growth factor signaling in fish. *Int Rev Cytol.*
685 243, 215–285.
686
687
688
689
690
691
692
693
694
695
696

697 **Figure legends**

698 **Figure 1.** Changes in Atlantic salmon myotubes in response to catabolic and anabolic treatments. (A)
699 Bright field images (a-d, i-l) or immunofluorescence against desmin filaments (e-h, m-p) is shown in
700 response to the +IL-1 β (a, e, i, m), -AA (b, f, j, n), +DEX (c, g, k, o) and +AA+Igf-I (d, h, l, p)
701 treatments after 48 hours. All pictures were taken at 20x magnification. The scale bars represent
702 150 μ m. (B) Changes in myotube diameter in response to -AA treatment vs. controls (+AA) and
703 +AA+IGF treatment. (C) Changes in myotube diameter in response to the +DEX treatment vs.
704 controls (-DEX). (D) Changes in myotube diameter in response to +IL-1 β treatment vs. controls (-IL-
705 1 β). Each box and whisker plot shows measurements from 100 to 150 myotubes. Significant
706 differences ($P < 0.05$) between controls and treatments are indicated at 24 hours (*), 48 hours (#) and
707 between -AA vs. +AA+IGF (+). The symbols '***', '###' and '+++' highlight differences at $P <$
708 0.001.

709
710 **Figure 2.** Significant mRNA-level expression responses to +DEX treatment for *igfbp6a1* (A),
711 *igfbp6b2* (B), *igfbp5a* (C), *igfbp5b1* (D), *igfbp4* (E), *igfbp2a* (F), *mafbx* (G), *murf1* (H), *igf2* (I) and
712 *atg4b2* (J) at 0, 1, 3, 6, 24 and 48 hours post-treatment showed as arbitrary units for controls (full bar
713 chart) and treated (empty bar chart) myotubes. Values for bar chart are mean + SD (n=5). Complete
714 details of gene expression responses for all genes tested in the study is provided in Table 1.

715
716 **Figure 3.** Significant mRNA-level expression responses to +IL-1 β treatment for *igfbp1a1* (A) and
717 *murf1* (B). All other details are as given in the Figure 2 legend. Complete details of gene expression
718 responses for all genes tested in the study is provided in Table 2.

719
720 **Figure 4.** Significant mRNA-level expression responses to -AA treatment for *igfbp6a1* (A), *igfbp6b2*
721 (B) and *mafbx* (C). All other details are as given in the Figure 2 legend. Complete details of gene
722 expression responses for all genes tested in the study is provided in Table 3.

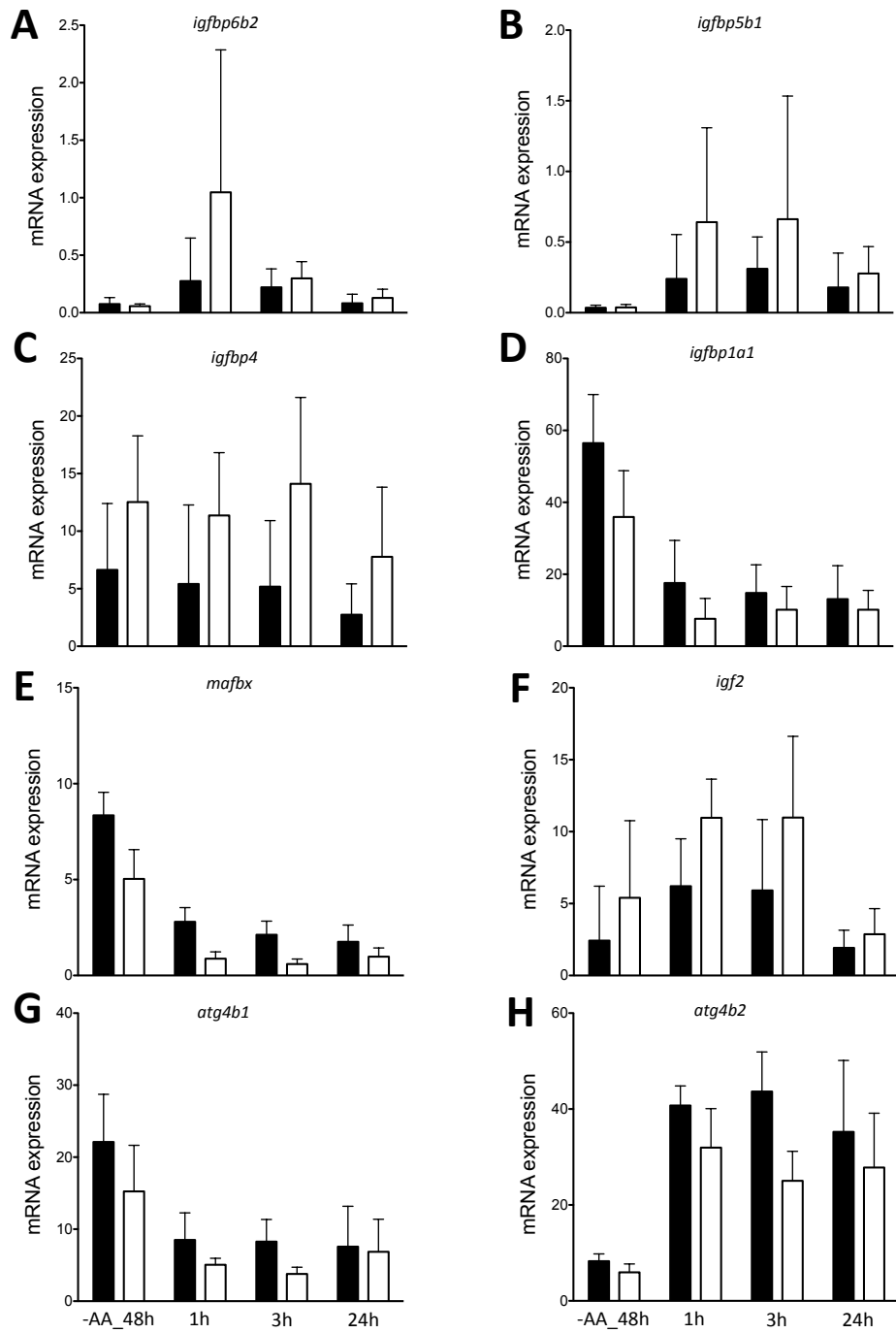
723

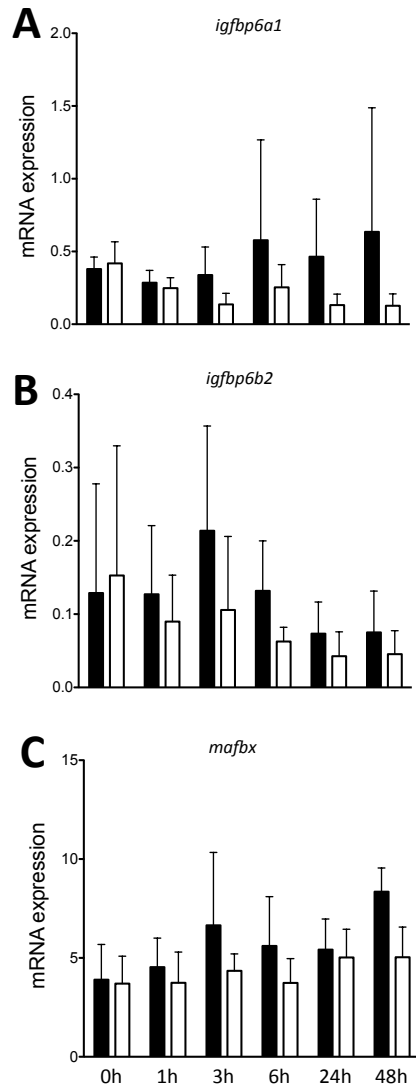
724 **Figure 5.** Significant mRNA-level expression responses to +AA+Igf-I treatment for *igfbp6b2* (A),
725 *igfbp5b1* (B), *igfbp4* (C), *igfbp1a1* (D), *mafbox* (E), *igf2* (F), *atg4b1* (G) and *atg4b2* (H) at 3, 6 and 24
726 hours post-treatment. All other details are as given in the Figure 2 legend. Complete details of gene
727 expression responses for all genes tested in the study is provided in Table 4.

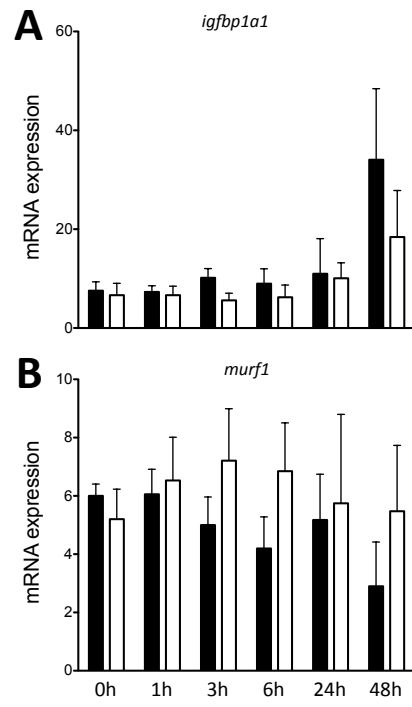
728

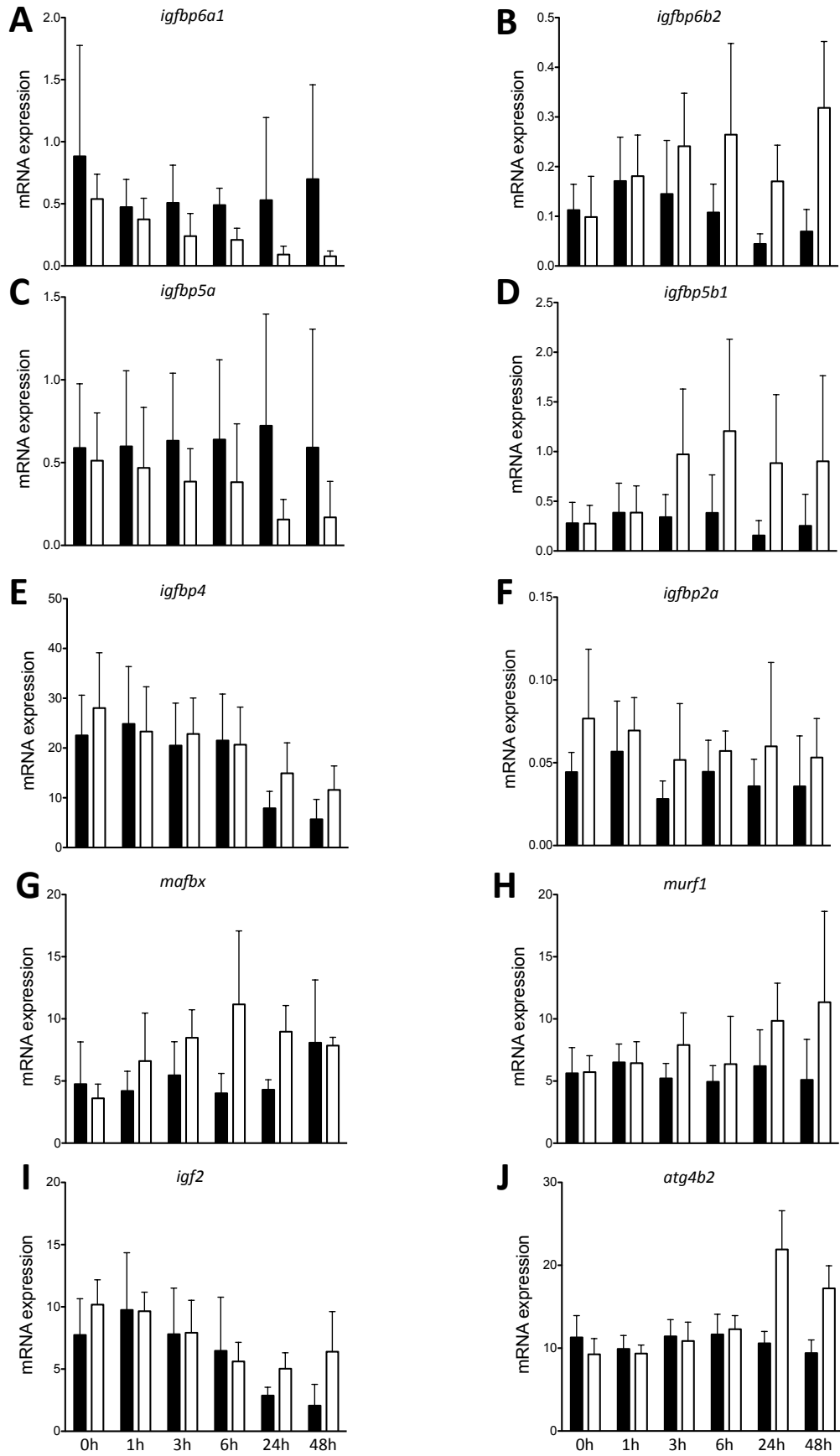
729 **Supplementary File 1.** Myotube morphology in response to catabolic and anabolic treatments.
730 Bright field microscopy or immunofluorescence against desmin (red) and actin (green) filaments for
731 myotubes under different experimental conditions. All pictures were taken using x20 magnification.
732 The scale bar for each picture represents 150µm.

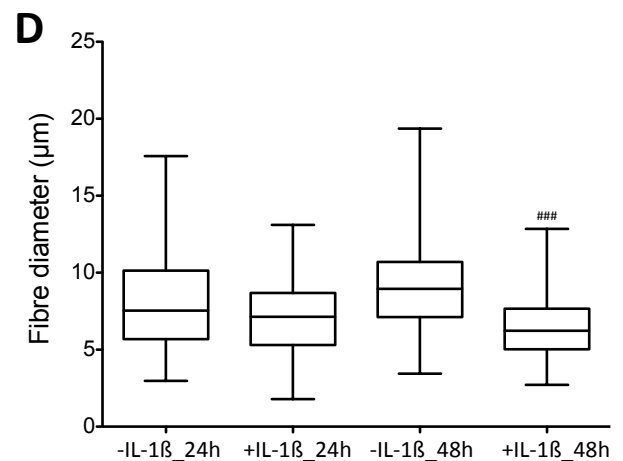
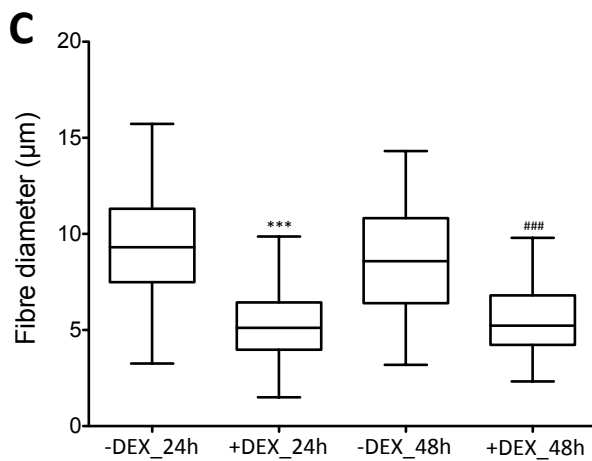
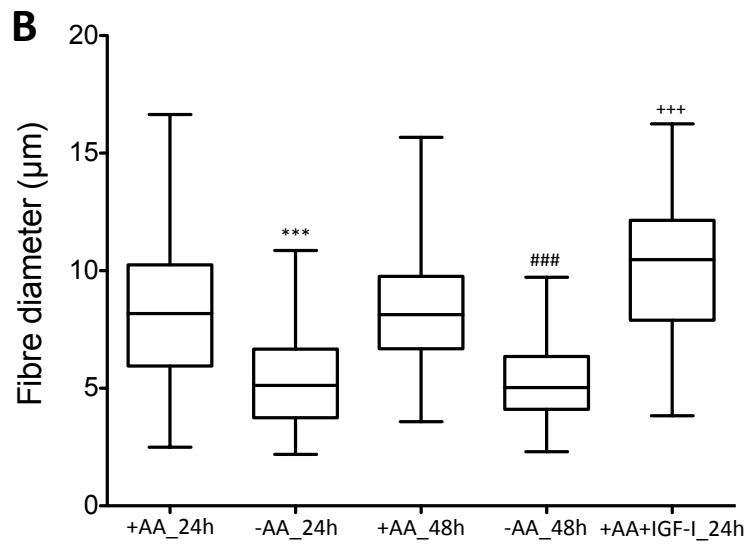
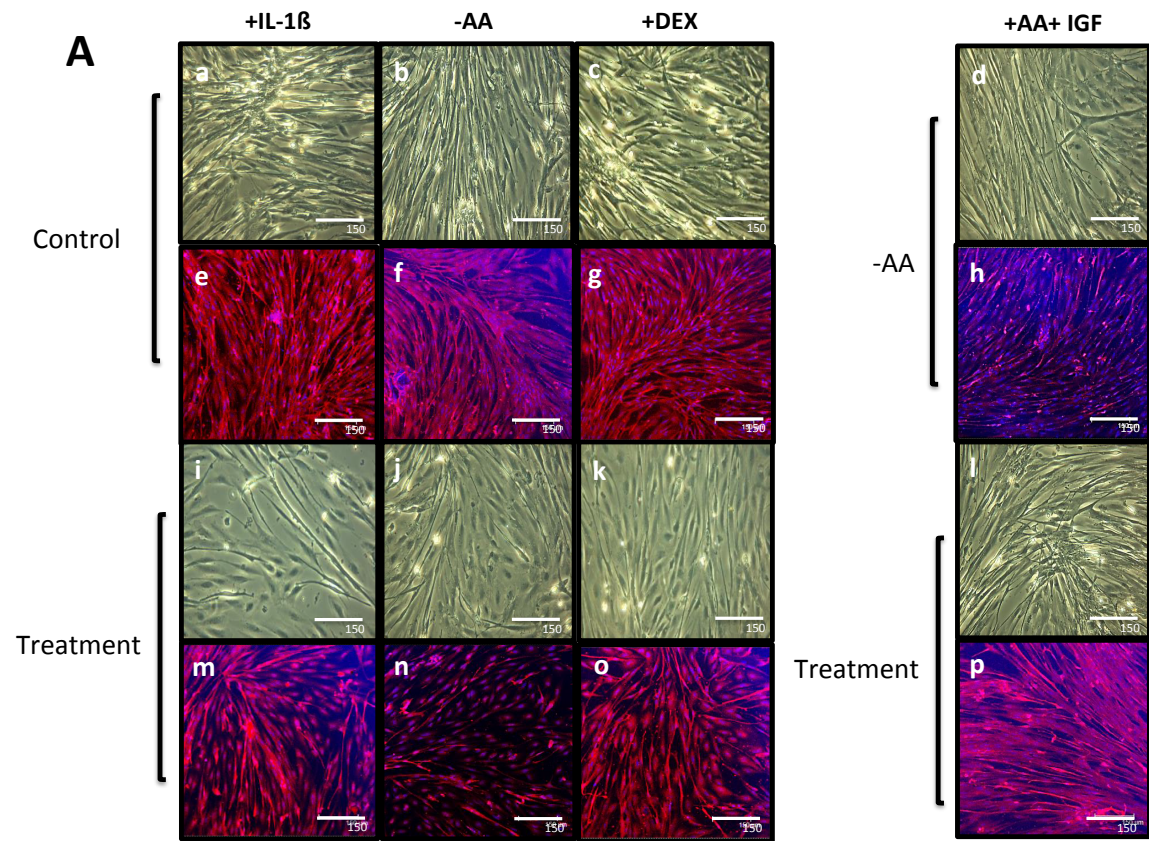
733











734

735

736

737 Table 1. Results of general linear modelling to investigate differences in gene expression in response to dexamethasone (+DEX) treatment

738

Gene	P-value Treatment	P-value Treatment *time-point	Transcript level 1 hour	+DEX / Control 1 hour	Transcript level 3 hour	+DEX / Control 3 hour	Transcript level 6 hour	+DEX / Control 6 hour	Transcript level 24 hour	+DEX / Control 24h	Transcript level 48 hour	+DEX / Control 48 hour
<i>igfbp6a1</i>	<0.0001	<u>0.032</u>	<u>0.37(0.17)</u>	<u>0.79</u>	<u>0.24(0.18)</u>	<u>0.47</u>	<u>0.21(0.09)</u>	<u>0.43</u>	<u>0.09(0.07)</u>	<u>0.17</u>	<u>0.08(0.04)</u>	<u>0.11</u>
<i>igfbp6b2</i>	<0.0001	0.005	0.18(0.08)	1.05	0.24(0.10)	1.66	0.26(0.18)	2.45	0.17(0.07)	3.83	0.31(0.13)	4.58
<i>mafbx</i>	<0.0001	<u>0.054</u>	<u>6.60(3.86)</u>	<u>1.57</u>	<u>8.47(2.25)</u>	<u>1.55</u>	<u>11.16(5.9)</u>	<u>2.78</u>	<u>8.96(2.10)</u>	<u>2.08</u>	<u>7.84(0.66)</u>	<u>0.97</u>
<i>murfl</i>	0.001	n/a	<u>6.44(1.72)</u>	<u>0.99</u>	<u>7.90(2.58)</u>	<u>1.51</u>	<u>6.36(3.83)</u>	<u>1.28</u>	<u>9.84(3.02)</u>	<u>1.58</u>	<u>11.3(7.31)</u>	<u>2.22</u>
<i>igfbp5b1</i>	0.002	n/a	<u>0.38(0.26)</u>	<u>1.00</u>	<u>0.97(0.65)</u>	<u>2.85</u>	<u>1.20(0.92)</u>	<u>3.14</u>	<u>0.88(0.68)</u>	<u>5.65</u>	<u>0.90(0.86)</u>	<u>3.56</u>
<i>igf2</i>	0.002	0.014	<u>9.65(1.52)</u>	<u>0.99</u>	<u>7.91(2.60)</u>	<u>1.01</u>	<u>5.61(1.53)</u>	<u>0.86</u>	<u>5.03(1.28)</u>	<u>1.75</u>	<u>6.39(3.22)</u>	<u>3.09</u>
<i>igfbp2a</i>	0.003	0.985	0.06(0.01)	1.22	0.05(0.03)	1.83	0.05(0.01)	1.28	0.05(0.05)	1.67	0.05(0.02)	1.48
<i>atg4b2</i>	0.003	<0.0001	<u>9.35(1.02)</u>	<u>0.94</u>	<u>10.8(2.28)</u>	<u>0.95</u>	<u>12.28(1.64)</u>	<u>1.05</u>	<u>21.9(4.66)</u>	<u>2.06</u>	<u>17.2(2.73)</u>	<u>1.83</u>
<i>igfbp5a</i>	0.007	0.443	<u>0.46(0.36)</u>	<u>0.86</u>	<u>0.38(0.19)</u>	<u>0.60</u>	<u>0.38(0.35)</u>	<u>0.59</u>	<u>0.15(0.12)</u>	<u>0.21</u>	<u>0.16(0.21)</u>	<u>0.28</u>
<i>igfbp4</i>	0.046	0.464	<u>23.3(9.00)</u>	<u>0.93</u>	<u>22.8(7.22)</u>	<u>1.11</u>	<u>20.6(7.55)</u>	<u>0.96</u>	<u>14.9(6.13)</u>	<u>1.89</u>	<u>11.5(4.81)</u>	<u>2.03</u>
<i>atg4b1</i>	0.100	0.082	13.0(2.96)	0.89	15.4(3.24)	0.91	21.4(5.20)	1.08	46.5(10.3)	1.56	43.0(7.94)	1.27
<i>igfbp3a1</i>	0.311	0.253	1.22(0.37)	0.89	0.95(0.32)	0.71	0.66(0.24)	0.51	0.98(0.53)	0.92	1.43(0.95)	1.24
<i>igfbp1a1</i>	0.464	0.814	14.2(4.29)	1.31	13.41(4.07)	1.19	12.9(5.56)	1.31	13.9(8.30)	0.85	28.8(16.8)	0.90
<i>igfbp5b2</i>	0.790	0.203	1.40(1.06)	1.05	2.37(1.90)	1.63	3.30(2.37)	1.80	1.03(0.50)	0.52	0.66(0.39)	0.17
<i>myll</i>	0.859	n/a	12.9(13.9)	0.87	15.1(14.0)	1.12	10.7(9.40)	0.71	8.95(10.3)	0.73	9.71(11.1)	1.54
<i>mn1l</i>	0.969	0.864	0.22(0.18)	0.81	0.28(0.18)	1.03	0.23(0.10)	0.88	0.34(0.29)	1.07	0.48(0.39)	1.81

739

740 Genes showing a statistically significant response to dexamethasone (+DEX) treatment are underlined.

741

742 All values where the +DEX treatment is divided by the control show fold change in transcript levels

743

744 n/a: treatment*time-point interaction not assessed (Kruskal-Wallis test applied)

745

746

747

748

746

747

748 Table 2. Results of general linear modelling to investigate differences in gene expression in response to interleukin 1 β (+IL-1 β) treatment

749

Gene	P-value Treatment	P-value Treatment *time-point	Transcript level 1 hour	+IL-1 β / Control 1 hour	Transcript level 3 hour	+IL-1 β / Control 3 hour	Transcript level 6 hour	+IL-1 β / Control 6 hour	Transcript level 24 hour	+IL-1 β / Control 24h	Transcript level 48 hour	+IL-1 β / Control 48 hour
<u><i>igfbp1a1</i></u>	<u>0.003</u>	<u>0.556</u>	<u>6.64(1.83)</u>	<u>0.90</u>	<u>5.59(1.45)</u>	<u>0.54</u>	<u>6.24(2.45)</u>	<u>0.69</u>	<u>10.1(3.12)</u>	<u>0.91</u>	<u>18.4(9.41)</u>	0.54
<u><i>murfl</i></u>	<u>0.004</u>	<u>0.124</u>	<u>6.53(1.48)</u>	<u>1.07</u>	<u>7.21(1.78)</u>	<u>1.44</u>	<u>6.84(1.65)</u>	<u>1.63</u>	<u>5.74(3.05)</u>	<u>1.11</u>	<u>5.47(2.26)</u>	1.88
<i>igfbp3a1</i>	0.128	0.796	0.87(0.34)	0.88	0.67(0.28)	0.51	0.49(0.06)	0.64	0.73(0.42)	1.09	0.55(0.29)	0.72
<i>igfbp6a1</i>	0.157	0.150	0.14(0.05)	0.83	0.24(0.18)	1.02	1.15(1.22)	2.22	0.79(0.43)	2.66	0.69(0.51)	1.39
<i>igfbp5b2</i>	0.181	0.955	0.90(0.63)	0.85	1.07(0.61)	0.47	1.50(0.83)	0.65	1.71(0.81)	1.05	1.47(0.87)	0.53
<i>atg4b1</i>	0.222	n/a	7.75(1.20)	0.89	8.73(0.93)	0.77	13.3(2.89)	0.86	22.3(7.94)	1.17	18.3(7.84)	0.87
<i>igfbp5b1</i>	0.284	0.675	0.27(0.14)	0.92	0.38(0.34)	1.02	0.46(0.48)	1.33	0.21(0.16)	1.39	0.17(0.14)	2.60
<i>igfbp4</i>	0.386	0.951	16.1(5.15)	0.92	13.9(4.09)	0.69	12.0(2.48)	0.95	7.41(4.5)	1.36	2.68(1.50)	0.73
<i>igfbp2a</i>	0.542	0.917	0.06(0.02)	0.88	0.05(0.02)	1.25	0.05(0.01)	0.99	0.05(0.02)	1.31	0.03(0.02)	0.97
<i>igfbp6b2</i>	0.581	0.695	0.10(0.07)	0.95	0.07(0.06)	0.41	0.07(0.05)	0.80	0.05(0.02)	0.76	0.05(0.02)	1.59
<i>mni1</i>	0.646	n/a	0.27(0.18)	1.05	0.26(0.16)	0.91	0.33(0.26)	1.23	0.38(0.28)	1.07	0.28(0.17)	0.93
<i>igf2</i>	0.680	n/a	5.97(3.74)	1.20	4.48(2.05)	0.72	2.64(1.13)	1.06	1.81(1.13)	1.26	1.30(0.39)	1.01
<i>atg4b2</i>	0.700	0.213	9.69(1.41)	0.97	10.3(0.71)	0.83	14.3(2.61)	1.05	12.9(5.14)	0.93	12.6(4.28)	1.14
<i>igfbp5a</i>	0.756	0.977	0.17(0.11)	1.14	0.24(0.18)	0.96	0.21(0.18)	1.31	0.15(0.09)	1.15	0.12(0.07)	0.53
<i>mafbx</i>	0.791	0.507	3.54(1.04)	1.09	4.02(0.88)	0.62	5.24(2.68)	1.13	4.80(1.88)	1.02	5.22(1.76)	0.79
<i>myll</i>	0.938	0.999	10.8(8.10)	1.03	10.8(8.45)	1.09	12.6(15.7)	1.60	8.59(8.30)	0.98	5.07(3.27)	1.17

750

751

752

753

754

755

Genes showing a statistically significant response to interleukin 1 β (+IL-1 β) treatment are underlined.
 All values where the +IL-1 β treatment is divided by the control show fold change in transcript levels
 n/a: treatment*time-point interaction not assessed (Kruskal-Wallis test applied)

757

758

759 Table 3. Results of general linear modelling to investigate differences in gene expression in response to amino acids deprivation (-AA) treatment

760

Gene	P-value Treatment	P-value Treatment *time-point	Transcript level 1 hour	-AA / Control 1 hour	Transcript level 3 hour	-AA / Control 3 hour	Transcript level 6 hour	-AA / Control 6 hour	Transcript level 24 hour	-AA / Control 24h	Transcript level 48 hour	-AA / Control 48 hour
<i>igfbp6a1</i>	<u><0.0001</u>	0.136	0.24(0.07)	0.87	0.13(0.07)	0.40	0.25(0.15)	0.43	0.13(0.07)	0.28	0.12(0.08)	0.20
<i>mafbx</i>	0.012	0.679	3.74(1.55)	0.82	4.34(0.87)	0.65	3.73(1.22)	0.66	5.02(1.42)	0.92	5.03(1.52)	0.60
<i>igfbp6b2</i>	0.039	0.747	0.08(0.06)	0.70	0.10(0.10)	0.49	0.06(0.02)	0.47	0.04(0.03)	0.58	0.04(0.03)	0.60
<i>igfbp5a</i>	0.056	n/a	0.26(0.19)	1.00	0.22(0.19)	0.68	0.28(0.28)	0.74	0.20(0.24)	0.60	0.06(0.08)	0.17
<i>murfl</i>	0.083	0.734	8.90(3.10)	1.19	9.85(1.64)	1.32	10.3(5.44)	1.26	8.14(3.20)	0.96	11.7(7.73)	2.07
<i>atg4b2</i>	0.092	0.569	8.06(1.58)	1.08	7.92(1.78)	0.97	7.14(3.26)	0.71	8.21(2.72)	0.74	5.95(1.74)	0.72
<i>igfbp3a1</i>	0.098	0.154	1.90(1.30)	0.88	1.68(0.52)	0.75	1.89(0.40)	1.14	3.61(1.84)	1.89	5.10(2.75)	2.35
<i>atg4b1</i>	0.107	0.744	9.56(3.54)	1.09	10.1(2.75)	0.94	10.6(3.18)	0.73	16.3(5.67)	0.68	15.2(6.40)	0.68
<i>myl1</i>	0.307	0.653	19.1(17.6)	1.38	16.4(16.0)	1.23	12.5(13.4)	0.78	7.00(8.06)	0.45	2.62(1.78)	0.43
<i>tnn1</i>	0.314	0.911	0.50(0.40)	1.19	0.40(0.25)	0.99	0.35(0.24)	0.72	0.38(0.37)	0.71	0.25(0.15)	0.73
<i>igfbp2a</i>	0.392	0.919	0.10(0.03)	0.97	0.07(0.02)	0.88	0.07(0.02)	1.12	0.05(0.02)	0.94	0.04(0.01)	0.72
<i>igf2</i>	0.409	0.504	5.94(5.64)	0.73	4.64(3.30)	0.63	6.33(4.68)	1.58	3.37(2.04)	1.25	5.39(5.36)	2.22
<i>igfbp1a1</i>	0.627	0.304	18.6(9.98)	0.94	17.84(7.92)	0.98	17.6(5.14)	1.11	25.4(9.43)	1.18	35.9(12.8)	0.63
<i>igfbp4</i>	0.649	n/a	30.2(20.7)	0.80	29.9(20.3)	0.84	31.8(18.9)	1.20	16.8(9.91)	1.38	12.5(5.74)	1.88
<i>igfbp5b1</i>	0.843	0.814	0.08(0.04)	0.94	0.100(0.08)	0.98	0.08(0.08)	0.56	0.06(0.05)	1.13	0.03(0.02)	1.06
<i>igfbp5b2</i>	0.901	0.994	0.50(0.57)	0.88	0.61(0.59)	0.74	1.38(1.14)	1.27	1.09(0.98)	1.24	1.15(1.06)	0.54

761

762

763

764

765

766

767

Genes showing a statistically significant response to amino acids deprivation (-AA) treatment are underlined.

All values where the -AA treatment is divided by the control show fold change in transcript levels

n/a: treatment*time-point interaction not assessed (Kruskal-Wallis test applied)

768

769

770 Table 4. Results of general linear modelling to investigate differences in gene expression in response to adding amino acids and Igf-I growth factor (+AA
771 +Igf-I) treatment.
772

Gene	P-value Treatment	P-value Treatment *time- point	Transcript level 48 hour*	+AA +Igf-I/ Control 48 hour*	Transcript level 1 hour	-AA / Control 1 hour	Transcript level 3 hour	-AA / Control 3 hour	Transcript level 24 hour	-AA / Control 24h
<i>mafbx</i>	<u><0.0001</u>	0.073	<u>5.03(1.52)</u>	0.60	<u>0.87(0.35)</u>	0.31	<u>0.59(0.26)</u>	0.28	<u>0.98(0.45)</u>	<u>0.55</u>
<i>atg4b2</i>	0.001	0.186	<u>5.95(1.74)</u>	0.71	<u>31.96(8.12)</u>	0.78	<u>25.03(6.15)</u>	0.57	<u>27.80(11.3)</u>	0.78
<i>igfbp4</i>	<u>0.002</u>	<u>0.888</u>	<u>12.5(5.74)</u>	<u>1.88</u>	<u>11.36(5.46)</u>	<u>2.09</u>	<u>14.1(7.5)</u>	<u>2.72</u>	<u>7.76(6.04)</u>	<u>2.82</u>
<i>igf2</i>	<u>0.009</u>	<u>0.824</u>	<u>5.39(5.36)</u>	<u>2.21</u>	<u>10.9(2.68)</u>	1.76	<u>10.9(5.64)</u>	<u>1.85</u>	<u>2.86(1.78)</u>	<u>1.49</u>
<i>igfbp6b2</i>	0.010	0.171	<u>0.05(0.01)</u>	0.75	<u>1.04(1.23)</u>	3.80	<u>0.29(0.14)</u>	1.35	<u>0.12(0.07)</u>	1.56
<i>igfbp5b1</i>	<u>0.016</u>	<u>0.354</u>	<u>0.03(0.02)</u>	<u>1.06</u>	<u>0.64(0.66)</u>	<u>2.67</u>	<u>0.66(0.87)</u>	<u>2.12</u>	<u>0.27(0.19)</u>	<u>1.54</u>
<i>igfbp1a1</i>	0.021	0.760	<u>35.0(12.8)</u>	0.63	<u>7.63(5.65)</u>	0.43	<u>10.1(6.46)</u>	0.68	<u>10.1(5.3)</u>	0.77
<i>atg4b1</i>	<u>0.033</u>	n/a	<u>15.2(6.24)</u>	0.68	<u>5.03(0.90)</u>	0.59	<u>3.78(0.92)</u>	0.45	<u>6.85(4.51)</u>	0.90
<i>igfbp5a</i>	0.086	n/a	<u>0.08(0.07)</u>	0.21	0.16(0.05)	1.46	<u>0.26(0.09)</u>	1.65	<u>0.12(0.07)</u>	4.84
<i>igfbp2a</i>	0.514	0.626	<u>0.04(0.01)</u>	0.72	<u>0.02(0.004)</u>	1.48	<u>0.02(0.01)</u>	1.47	<u>0.02(0.009)</u>	1.43
<i>murf1</i>	0.608	0.057	<u>11.78(7.73)</u>	2.07	<u>3.59(1.28)</u>	0.81	<u>2.16(1.33)</u>	0.61	<u>3.33(1.33)</u>	0.69
<i>tnn1</i>	0.689	0.534	<u>0.25(0.15)</u>	0.73	<u>0.27(0.18)</u>	0.77	<u>0.27(0.19)</u>	0.76	<u>0.99(0.71)</u>	1.84
<i>igfbp5b2</i>	0.834	0.404	<u>1.15(1.06)</u>	0.54	<u>0.20(0.21)</u>	0.96	<u>0.15(0.10)</u>	0.71	<u>0.58(0.48)</u>	1.88
<i>igfbp3a1</i>	0.875	0.063	<u>5.10(2.75)</u>	2.35	<u>1.03(0.68)</u>	1.44	<u>0.65(0.34)</u>	0.85	<u>0.47(0.25)</u>	0.74
<i>igfbp6a1</i>	0.877	0.029	<u>0.12(0.08)</u>	0.20	<u>0.12(0.04)</u>	0.84	<u>0.32(0.27)</u>	2.30	<u>0.66(1.09)</u>	4.24
<i>myl</i>	0.879	n/a	<u>2.62(1.78)</u>	0.43	<u>8.98(12.75)</u>	0.95	<u>12.8(18.4)</u>	1.19	<u>13.5(15.2)</u>	0.98

773

774

775

776

777

778

779

* refers to myotubes being maintained for 48 hours in media free of amino acids for 48 hour before adding amino acids and Igf-I growth factor (+AA +Igf-I) treatment

Genes showing a statistically significant response to +AA +Igf-I treatment are underlined.

All values where the +AA +Igf-I treatment is divided by the control show fold change in transcript levels

n/a: treatment*time-point interaction not assessed (Kruskal-Wallis test applied).